Supplement of Earth Surf. Dynam., 12, 1165–1191, 2024
https://doi.org/10.5194/esurf-12-1165-2024-supplement

Earth Surface Dynamics
Open Access
EGU

Supplement of

A landslide runout model for sediment transport, landscape evolution, and hazard assessment applications

Jeffrey Keck et al.

Correspondence to: Jeffrey Keck (keckje@gmail.com)

Contents

1. Additional information on field and remote sensing observations

In the field, we walked the runout path from the head of the landslide to the terminus of the runout deposit noting the location and thickness of deposition and erosion, deposit composition, the slope of channel-filling deposits and maximum grain sizeof the runout material. Geometric measurements in the runout path were measured using a combination of a clinometer, steel tape and range finder. Location was measured using a handheld GPS with maximum accuracy = +/- 1.8 m. Maximum grain size (which at all sites was cobble to boulder sized) was visually approximated in the field or from photos that included a scale object, to the nearest 5 cm at eight to sixteen points along the runout path. We estimated deposition depth from the thickness of fluvially eroded terraces and burial depth of stumps or trees. In channels that were eroded to the fresh bedrock surface, we estimated erosion depth using the regolith thickness visible along the edges of scoured channel walls (Olympic Mountains). At locations where erosion was limited to within the regolith, we used vegetative indicators such as the remnants of in-situ tree roots (Rocky Mountains) and the adjacent, uneroded regolith surface to estimate erosion depth.

Remote observations included air photos (DNR, 2022; Google Earth, 2022) and lidar DEMs (DNR, 2022; Open Topography, 2022) of the landslide and runout path. The lidar DEMs were used to define the model domain. The air photos were used in combination with field observations and the lidar DEM to interpret the lateral extent of the observed runout. Where

pre- and post-mass wasting event lidar DEMs were available, we subtracted the pre-event DEM from the post-event DEM to create the DoD. We found that not all DEMs or regions of the DEM were of equal quality and therefore, where possible, DoD maps derived from lidar differencing were checked in the field. At sites with only one post-event lidar DEM (Rocky Mountains and Olympic Mountains), we created DoD entirely from field observations of deposition and erosion. Model setup details specific to each site are detailed below.

2. Observed runout and model setup

Cascade Mountains

Site and mass wasting runout description

The Cascade Mountains site includes two landslides that occurred in 2009 and 2022, one in each year, on a hillslope located roughly 30 km south of Mount St. Helens, USA, near the south-west edge of Washington State. The hillslope is moderately steep (average slope ~40 to 60%), broadly convergent and dissected by a small, first-to-second order channel. The 2022 landslide was a reactivation of the 2009 landslide headscarp. Two logging roads cross the hillslope and impacted flow behavior, particularly during 2022 event. The underlying regional geology is Miocene-Oligocene volcaniscalistic deposits or rocks (DNR, 2022), which in the field consisted of hydrothermally altered basaltic andesite and epilcastic sandstone with gravel to cobble intrusions. In some areas, the rock was weathered to clay and rippable with a hand shovel. During both events, the runout path was covered in trees, though the size and age of the trees differed.

Both landslides were triggered during heavy rain-on-snow precipitation events (Table 1). For both landslides, overall runout extended 700 to 800 meters downslope from the base of the landslide, ending abruptly when the runout perpendicularly intersected a narrow river valley at the base of the hillslope. The first event was a large, catastrophic debris avalanche (initial landslide volume = 110,000 m^3) that flowed relatively unconfined over a wide area of the downslope hillslope, completely inundating the small, first-to-second order channel. At the time of the 2009 event, 0.6 to 0.9 meter diameter conifer trees covered the hillslope. The 2009 event obliterated the logging roads and all trees in the runout path. Roughly 29% of the total mobilized volume was derived from erosion during the runout.

The second event was smaller than the 2009 event, but was still moderate in size (initial landslide volume = 22,000 m^3). By 2022, the roads were reconstructed and the 2009 scar was covered with small (0.1 to 0.2 diameter) hardwood trees. Runout of the second event was largely confined to the small, first-to-second order channel in the center of the scar of the 2009 slide, forming a channelized debris flow and destroying most of the small hardwood trees in its path. Unlike the 2009 event, except for a ~3m wide area of erosion in the upper road, both the upper and lower road remained intact and acted as a check-dam. Roughly 19% of the total mobilized volume was derived from erosion during the runout.

In the field (March, 2022), deposits consisted of a mixture of 70 to 80% clayey sand matrix with 20 to 30% gravels and cobbles and trace boulders. The slope of areas of positive net deposition ranged from 5 to 15% but slopes as low as 1% may have formed along the lower river valley (Table 1). Along the margins of the runout path, hummocky, cohesive levees formed on a range of slopes (See Figure S1b).

Observed-runout dataset and model setup

At this site, we have high-resolution DEMs of the terrain before and after each runout event: a 2-meter Lidar DEM recorded in 2006, a 1-meter Lidar DEM recorded in 2019, and a structure-from-motion DEM of the runout path created from unmanned aerial vehicle images, recorded in 2022. The 2019 DEM was recorded before reconstruction of the upper logging road and thus does not accurately represent the topography at the time of failure in 2022. We added the upper road to the 2019 Lidar DEM using AutoCAD Civil3D based on the engineer's design drawings.

We used the 2006 DEM as the pre-event terrain for the 2009 event and the modified 2019 DEM as the pre-event terrain for the 2022 event. We created the map of observed $\Delta\eta$ (DoD) for the 2009 event by subtracting the 2006 DEM from the unmodified 2019 DEM and for the 2022 event by subtracting the modified 2019 DEM from the 2022 DEM. Because the 2019 DEM was recorded nearly 10 years after the 2009 event, by the time the 2019 DEM was recorded, much of the deposit near the channel in the center of the runout path and most of the deposit in the river valley appears to have been fluvially eroded. Also, the lower road was reconstructed. For the 2022 event, most of the runout material was still in-place when the 2022 DEM was recorded.

For the model setup, we used a 10-m grid size. We assumed an average erodible regolith of 1.2 meters based on the depth of regolith visible in road cuts and the average observed erosion depth. Because much of the 2009 deposit in the river valley was eroded after the event and no longer represented in the 2019 DEM, we limited the comparison of Q_s to the hillslope above the lower river valley, which corresponded to roughly the first 750 meters of the runout path (measured from the landslide crown).

Black Hills

Site and mass wasting runout description

The Black Hills landslides occurred in 2007, in adjacent, east-west oriented basins, in response to an extreme precipitation and snowmelt event (Table 1). The southern basin has an area of 2 km^2 and is drained by a second order channel. The northern basin has an area of 2.8 km^2 and is drained by a third order channel. Logging roads cross both the headwater and the outlet of the basins. Underlying geology is weathered basalt covered by a thick regolith that includes a deep

(2 to 5 meters) saprolite layer of clay-rich soil with occasional cornerstones of basalt and exotic, glacially derived clasts (DNR, 2022).

In the southern basin, a deep-seated bedrock landslide partially mobilized on a moderately steep slope (40%) but came to rest upon intersecting the channel that runs along the center of the basin. A small portion of the toe of the landslide broke off (initial landslide volume ~1,500 m^3) in the channel and continued flowing until reaching the logging road at the mouth of the basin. In the northern basin, a moderately sized landslide (initial landslide volume ~ 18,500 m^3) catastrophically failed in the through-fill section of a logging road, located 250 meters upslope of the channel on a 60% slope (vertically 150 meters higher than the channel). Based on super elevation of the flow, evident in the elevation of scour and mud marks on the left and right sides of the runout path, flow velocity was high. Despite differences in initial landslide velocity near the top of the runout path, over most of the runout path, both landslides progressed down relatively low-gradient channels as debris flows, eroding and entraining debris and large trees (0.2 to 0.7 meters) until eventually depositing near the junction of a larger channel. The total mobilized volume derived from erosion during the runout was 89% and 59% at the southern basin and northern basin respectively.

In the field (December, 2021), the runout deposit in the southern basin consisted of 65% sandy silt matrix with 35% gravels. In the northern basin, the runout deposit consisted of 45% sandy matrix with 55% gravels. The slope of positive net deposition deposits measured in the field ranged from <1 to 10%. Most of the entrained woody debris was transported to the end of the runout path where it deposited as large, 2 to 3 meter high stacks of logs. Some woody debris did deposit at higher locations in the channel, which in turn caused sediment to deposit on relatively steep reaches of the channel.

Observed-runout dataset and model setup

Here we have a 2-meter DEM recorded in 2005 and a 1-meter DEM recorded in 2011. We had to translate the 2005 DEM vertically roughly 0.5 m to get rid of a systematic offset with the 2011 dataset. We created the observed-runout dataset by subtracting the translated 2005 DEM from a 2-meter resampled version of the 2011 dataset. Much of the 2005 DEM appears to include occasional fragments of the vegetation surface, but in the valley bottom, near the channel, the DEM generally appears smooth and a better representation of the ground surface. Nonetheless, we use the 2005 translated Lidar DEM, resampled to a 10-meter grid and smoothed using a low-pass filter (ArcGIS, 2022) to remove vegetation interference as the pre-event terrain and we field verified areas of scour or deposition signals in the DoD. Similar to 2019 DEM at the Cascade Mountains site, areas of deposition appear to have been fluvially eroded between the pre-and post-event DEM. At this site, we assumed an average erodible regolith depth of 1.5 meters.

Rocky Mountains

Site and mass wasting runout description

The Rocky Mountains landslide occurred in September, 2013, following an intense period of rainfall (Patton et al., 2016) on a steep, broadly convergent to divergent hillslope. It was a moderately sized debris avalanche (initial volume ~4600 m^3) sourced from thick (>6 m) colluvium. The area is underlain by gneiss, schist, migmatite and Proterozoic granites (USGS, 2022). In the field (August, 2022), bedrock was generally covered by thick colluvium, which consisted of a sandy, gravel matrix mixed with cobbles and very large boulders (diameter > 2 meters). Evidence of macropore-flow and infiltration-excess surface runoff were visible in the headscarp. The only water available to mix with the landslide debris appears to have been limited to these runoff sources as the majority of the runout path does not follow a channel.

The hillslope below the landslide is planar and moderately steep (40 to 50 %) for about 350 meters and then transitions to a 20 to 30 %, broadly divergent slope. At the time of the failure, the hillslope was densely forested with 0.2 to 0.4-meter diameter conifer trees with rooting depths of about 0.5 to 1 m. Most erosion occurred on the planar hillslope and removed the upper 0.5 to 1 m of colluvium (inferred from the tips of tree roots visible in areas of erosion) but channelized erosion as deep as 4 to 5 meters also occurred.

Unlike the other validation sites, as the debris flowed from the landslide to the lower extent of the runout path, it spread laterally. Also, here, vegetation, rather than convergent topography, appears to have largely controlled the lateral extent of the flow. Along the edge of the runout path, a nearly continuous berm of logs developed as the mobilized material flowed down slope (see Figure S1c).

Positive net deposition began at gradient of 16 to 25%, near the slope break between the planar slope and the divergent slope. Once on the divergent hillslope, the runout split, with a small lobe of material flowing northwest, and the majority of the material flowing southwest. Relative to the other sites, deposited material near the slope break was unusually well sorted and thick (2-3 meters). Deposited material on the northwest lobe was mostly fine gravel to sand sized and deposition depths were relatively shallow (roughly 10 to 30 cm). Material that flowed to southwest included many large boulders, which deposited just downslope of the thick gravel deposit. A thin (0.2 to 0.5 meter) sand and fine gravel deposit continued past the boulders. An eyewitness account of the deposit shortly after the runout described the terminal end of the runout as a mudflow. The average composition of observed deposited material was 40% sandy gravel matrix with 60% gravels, cobbles and boulders. Here, 88% of the total mobilized volume was derived from erosion during the runout but the runout was not long, which resulted in an extreme growth factor of 95 m^3/m of channel length.

Observed-runout dataset and model setup

Here we only have one, post-event Lidar dataset, recorded in 2015. We rely on field observations of erosion and deposition depths to approximate the DoD. We used in-place tree roots in the runout-scar and adjacent, intact topography to estimate changes in elevation within the runout path. Scour depths and deposition depths were generally shallow (<1.5 m). Where deep scour occurred, it was localized to narrow channels, that may have formed after the runout event. At this site, we assumed an average erodible regolith depth of 1.2 meters. We approximated a pre-event DEM by subtracting the field estimated map of $\Delta\eta$ from the post-event DEM, resampling to a 10-meter grid cells and smoothing the DEM using the same low pass filter we applied to the Black Hills 2005 DEM.

Olympic Mountains

Site and mass wasting runout description

The Olympic Mountains site is a small (2.1 km^2), dendritic, fourth order basin. Inspection of the air photo record revealed that over a 30 year period (1980 and 2010), at least twelve small (initial landslide volume ~ 400 to 2200 m^3) landslides initiated along the edges or heads of a first or second order channels and subsequently formed channelized debris flows. Between 1980 and 2010, at least six different precipitation events with 2-day precipitation totals between 100 and 220 mm occurred (Table 1).

The basin is underlain by Miocene-Eocene marine sedimentary rocks (WA DNR, 2022), which in the field appear as steeply bedded densely fractured 1 to 2-meter thick beds of siltstone with occasional beds of 0.3 to 0.5-meter beds of coarse grained sandstone. These beds generally break up into 10 to 30 cm sized clasts, though boulders larger than half a meter in diameter are also common, with most of the larger clasts derived from the sandstone. Many of the channels were filled with thick colluvial deposits that predated the debris flows triggered after 1980.

Approximately 60% of basin area was logged and replanted between 1978 and 1990. At the time of most debris flows, valley bottoms were not vegetated but logs left from the tree harvests cluttered the channel. Here, few roads were constructed in the watershed and, except for a small landslide (~100 m^3) that initiated from the fillslope of a road, roads appear to have had little impact on mass-wasting processes.

In the field (March, 2021), debris flow deposits were visible throughout the channel network and consisted of 40% sandy-gravel matrix with 60% coarse gravels, cobbles and boulders. The surface slope of reaches of positive net deposition generally systematically increase in the upstream direction from ~5% near the basin outlet to 15% at the upper extent of deposition (Table 1). Several deposits formed behind thick log jams (Figure S1a), which restricted the runout distance of some flows. At this slide, 97% of the total mobilized material consisted almost entirely of eroded and entrained material but because runout occurred over long distance in relatively narrow channels, the growth factor is relatively low (Table 1). Soil depth visible in tree-throw pits within the basin varied from 1 to 1.5 m but is as deep as 3 m on lower-

gradient alluvial and colluvial deposits. Here, we defined soil depth as a function of contributing area, slope gradient and the minimum and maximum field-observed soil depths following Westrick (1999).

Observed-runout dataset and model setup

Here we have a 2005, Lidar DEM, recorded after most of the landslides occurred (post-event). Like the Rocky Mountains site, we relied on field observations of erosion and deposition depths to approximate the DoD. Many of the deposits were fluvially eroded but the original extent and elevation of the deposit could be identified by terraces of material left along the channel wall. At this site, the landslides were relatively small and the resulting runout deposits appeared to only add a new layer to pre-existing valley-filling debris flow deposits without changing the valley slope. We therefore used the 2005 DEM resampled to a 10-meter grid, as the pre-event DEM.

3. LandslideProbability setup

We setup LandslideProbability using soil strength and hydrologic parameters based on the soil class (SSURGO, 2020) and vegetation type following Strauch et al. (2018). We defined soil depth as a function of contributing area, slope gradient and minimum and maximum depths following Westrick (1999). Minimum and maximum soil depths were estimated from field observations at channel banks, tree-throw pits and road cuts. For recharge, we assumed evapotranspiration and soil storage losses were small, and used a spatially uniform daily precipitation depth equivalent to the 50 year event (determined from rainfall records; WRCC, 2017).

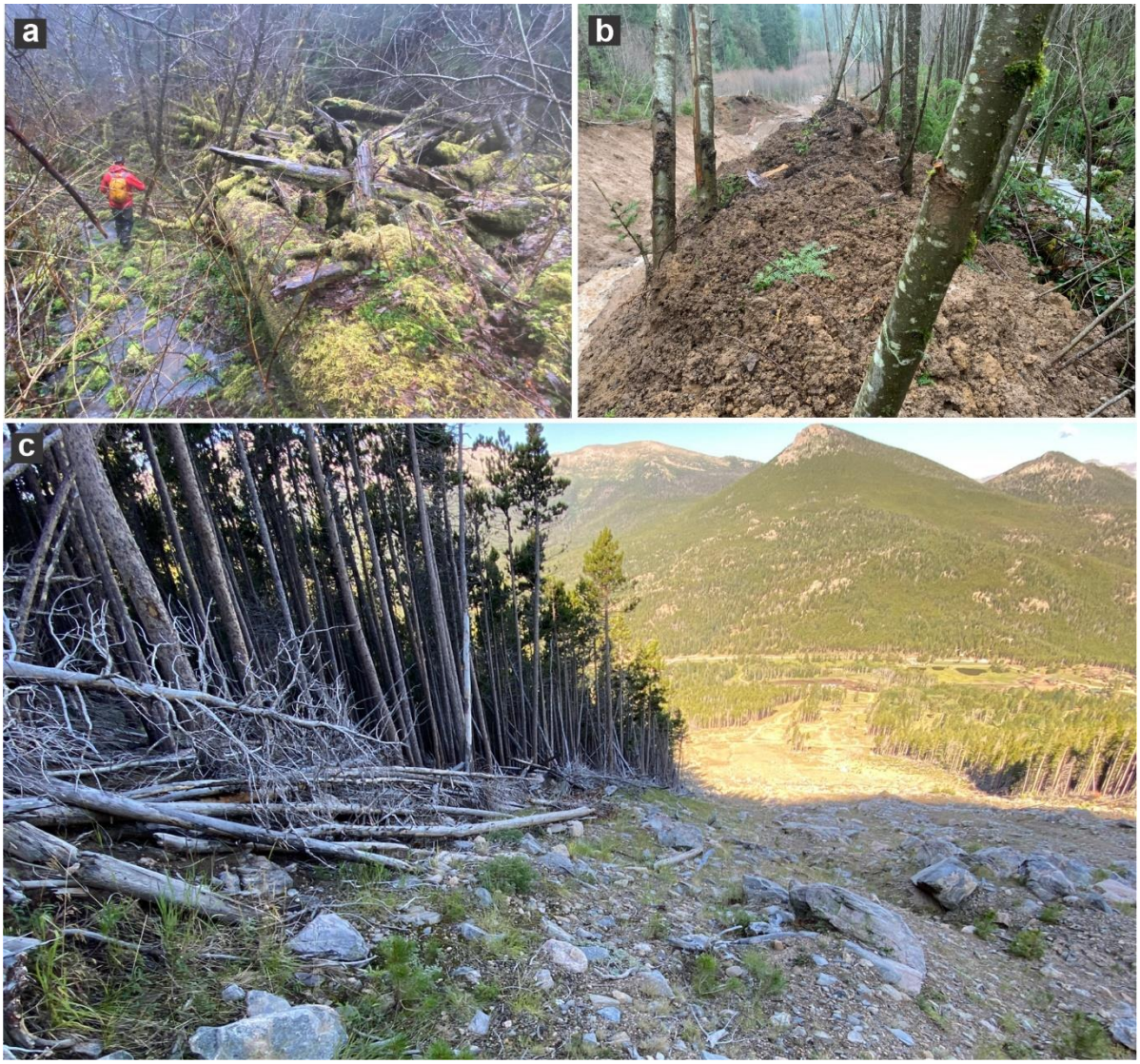

Figure S1 Example woody debris impact on observed runout behavior. **(a)** Wood jams at the Olympic Mountains site that caused valley-filling deposits. **(b)** Small, standing hardwood trees resisted relatively shallow flow along the margins of the runout material to form levees. (photo credit: John Jenkins). **(c)** Woody debris piled along the edge of the flow and controlled lateral spreading at the Rocky Mountains site.

4. References

1. Google Earth, https://earth.google.com/, accessed 2022 and 2023
2. OpenTopography, https://opentopography.org/ accessed August, 2022

3. Patton, A. I., Rathburn, S. L., Bilderback, E. L., & Lukens, C. E.: Patterns of debris flow initiation and periglacial sediment sourcing in the Colorado Front Range. Earth Surface Processes and Landforms, 43(15), 2998–3008. https://doi.org/10.1002/esp.4463, 2018.
4. SSURGO Database | Natural Resource Conservation Service , United States Dept. of Agriculture, https://www.nrcs.usda.gov/resources/data-and-reports/soil-survey-geographic-database-ssurgo, accessed September, 2022
5. WA DNR geology portal, https://www.dnr.wa.gov/geologyportal, accessed June, 2022
6. WA DNR, Department of Natural Resources, https://www.dnr.wa.gov/programs-and-services/buy-maps-aerial-photos-or-survey-data
7. Western Regional Climate Center. (n.d.). Retrieved 2017, from https://wrcc.dri.edu/
8. Westrick, K.: Soil depth calculation script implemented in python. Retrieved from https://github.com/pnnl/DHSVM-PNNL, 1999.
9. Western Regional Climate Center. (n.d.),https://wrcc.dri.edu/, accessed 2017